



Divergence time and environmental similarity predict the strength of morphological convergence in stick and leaf insects

Romain P. Boisseau^{a,b,1}, Sven Bradler^c, and Douglas J. Emlen^{a,1}

Affiliations are included on p. 11.

Contributed by Douglas J. Emlen; received November 6, 2023; accepted November 4, 2024; reviewed by Scott V. Edwards and Jonathan B. Losos

Independent evolution of similar traits in lineages inhabiting similar environments (convergent or repeated evolution) is often taken as evidence for adaptation by natural selection, and used to illustrate the predictability of evolution. Yet convergence is rarely perfect for two reasons. First, environments may not be as similar as they appear. Second, responses to selection are contingent upon available genetic variation and independent lineages may differ in the alleles, genetic backgrounds, and even the developmental mechanisms responsible for the phenotypes in question. Both impediments to convergence are predicted to increase as the length of time separating two lineages increases, making it difficult to discern their relative importance. We quantified environmental similarity and the extent of convergence to show how habitat and divergence time each contribute to observed patterns of morphological evolution in 212 species of stick and leaf insects (order Phasmatodea). Dozens of phasmid lineages independently colonized similar habitats, repeatedly evolving in parallel directions on a 23-trait morphospace, though the magnitude and direction of these shifts varied. Lineages converging toward more similar environments ended up closer on the morphospace, as did closely related lineages, and closely related lineages followed more parallel evolutionary trajectories to arrive there than more distantly related ones. Remarkably, after accounting for habitat similarity, we show that divergence time reduced the extent of convergence at a constant rate across more than 100 My of separation, suggesting even the magnitude of contingency can be predictable, given sufficient spans of time.

Phasmatodea | ecomorph | repeated evolution | homoplasy | macroevolution

When does convergent evolution happen? Examples of lineages independently evolving similar phenotypes are numerous and conspicuous (also referred to as “repeated evolution”) (1–5) [e.g., gliding mammals (6), cave amphipods (7, 8), Hawaiian spiders (9)], and likely result from adaptation to similar ecological niches [(3, 9, 10), but see ref. 11]. Yet convergence is rarely perfect and sometimes does not occur at all, even when habitats are similar. When it does occur, the extent of phenotypic similarity varies widely (6, 10, 12) and the factors causing this variation and, by extension, influencing the repeatability of evolutionary outcomes, are not well understood (13, 14).

One important determinant of the likelihood and extent of convergent evolution is the degree of relatedness among lineages. Repeated evolution usually involves closely related taxa (11) [e.g., Caribbean *Anolis* lizards (15, 16), three-spined stickleback fish (17)], suggesting that strong convergence is most likely when the time separating lineages is brief [i.e., phylogenetic bias (14)]. Gould famously argued that evolutionary outcomes are contingent on the intricate series of historical events uniquely experienced by each lineage (18–20). Closely related lineages share more of their evolutionary history and, consequently, more of their genetic variation (17, 21–26). They are also more likely to share the same ancestral niche and associated ancestral phenotypes (13). Three-spine stickleback repeatedly colonized lakes and streams from the same marine habitat, for example (21, 27). In these instances, adaptation to the new niche is likely to proceed through similar sequences of phenotypic changes [i.e., parallel or collinear evolutionary trajectories (5)] arriving at phenotypes that are strongly resemblant. More disparate lineages may approach a shared environmental challenge from different starting phenotypes, with weaker convergence as a result. And lineages with enough accumulated differences may not converge at all. Aye-ayes (Primates) and woodpeckers (Aves) each catch and eat insect larvae found under the bark of trees, yet they forage in strikingly different ways (13). Aye-ayes use their teeth to break through the bark and

Significance

Phasmids (stick and leaf insects) exemplify the extraordinary power of natural selection to shape organismal phenotypes. The animals themselves are charismatic exemplars of crypsis and masquerade; and our characterization of their adaptive radiation reveals dozens of instances of convergence, as lineages adapted to similar changes in habitat by repeatedly evolving similar body forms. Our findings show that the similarity of environmental conditions experienced by the organisms—the closeness of the invaded niches—and the extent of elapsed time since divergence, both predict the strength of morphological convergence. The phasmid radiation reveals an evolutionary process that is surprisingly predictable, even when lineages have been evolving independently for tens of millions of years.

Author contributions: R.P.B., S.B., and D.J.E. designed research; R.P.B. performed research; R.P.B. analyzed data; S.B. curated and contributed specimens; and R.P.B. and D.J.E. wrote the paper.

Reviewers: S.V.E., Harvard University; and J.B.L., Washington University in St. Louis.

The authors declare no competing interest.

Copyright © 2024 the Author(s). Published by PNAS. This article is distributed under [Creative Commons Attribution-NonCommercial-NoDerivatives License 4.0 \(CC BY-NC-ND\)](https://creativecommons.org/licenses/by-nc-nd/4.0/).

¹To whom correspondence may be addressed. Email: romain.boisseau@unil.ch or doug.emlen@mso.umt.edu.

This article contains supporting information online at <https://www.pnas.org/lookup/suppl/doi:10.1073/pnas.2319485121/-/DCSupplemental>.

Published December 23, 2024.

an elongated middle finger to catch larvae, while woodpeckers use hammering beaks to get through the bark and long, barbed tongues to catch insects.

Consequently, the extent of shared evolutionary history and the similarity of phenotypic ancestral states should each affect the likelihood of repeated phenotypic evolution. Specifically, the lower the opportunity for contingency—less accumulated time since their split—the more likely any two lineages should be to converge strongly in response to a shared selection environment. A 2015 meta-analysis supported this prediction: Convergent evolution was more likely to be documented among closely related than distantly related taxa, particularly when considering morphology (11). This pattern also holds at the molecular level, as the degree of gene reuse decreases with divergence time when lineages repeatedly adapt to similar environments (23–26, 28), or evolve analogous individual traits (22). Yet explicit tests of Gould’s predicted link between divergence time and the extent of phenotypic convergence are lacking.

Quantifying the role of divergence time on convergence requires a system i) where the extent of phenotypic convergence and environmental similarity can be quantified precisely; ii) where instances of convergence span vast periods of time from recently diverged to much more distantly genetically related lineages; and iii) where there are enough instances of convergence to allow sufficient statistical power. Here, we use the morphological diversity of stick and leaf insects (order Phasmatodea, ~3,500 described species) to provide such test. Most species exhibit stunning forms of camouflage through background matching [crypsis (29)] and the mimicry of objects irrelevant to predators [masquerade (30)] such as sticks, leaves, bark pieces, or moss (31–33). Selection to match such diverse objects produced a spectacular morphological diversity ranging from elongated tubular bodies with long slender legs to bodies so wide and flattened they look like leaves (Fig. 1). Recent phylogenetic studies of phasmids conflict with prior taxonomic classifications based on morphological characters, suggesting a high degree of morphological convergence across the

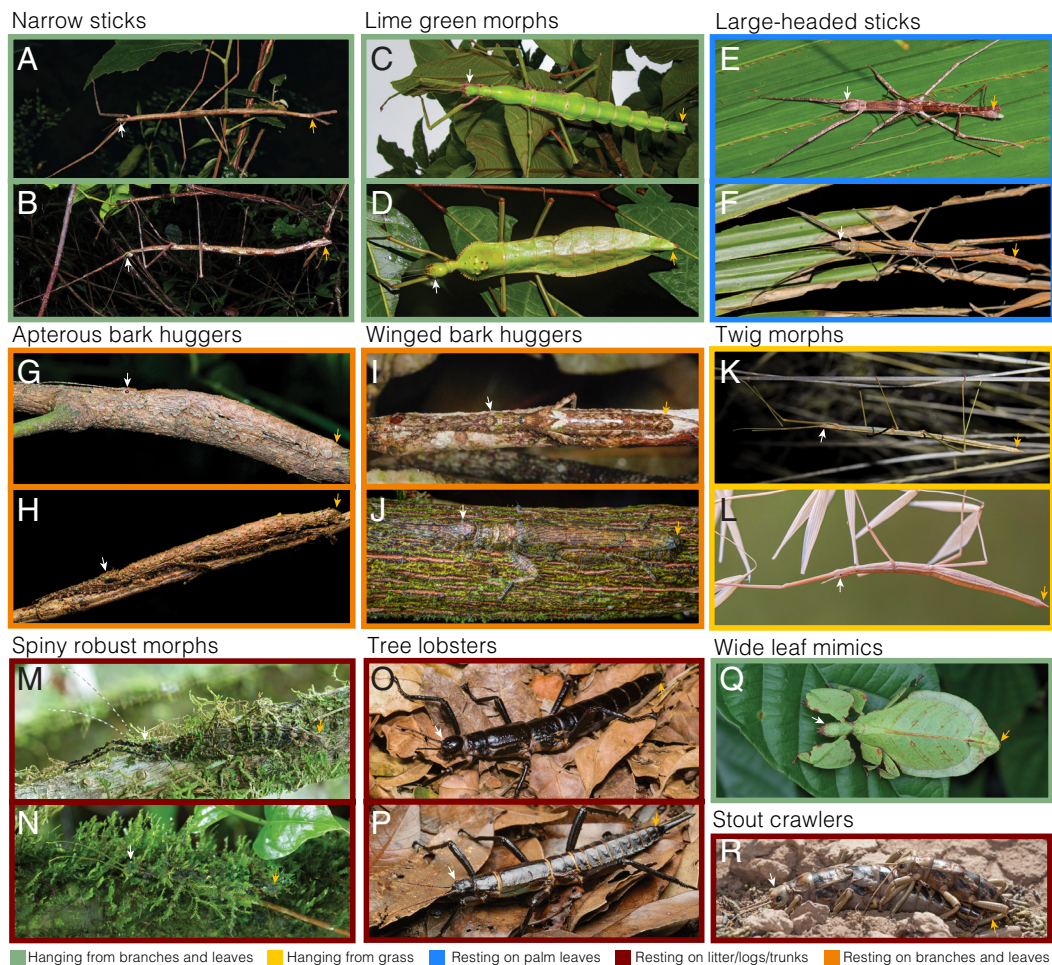


Fig. 1. Photographs of adult females in situ. The color surrounding each picture corresponds to a habitat use category. White arrows point to the head, orange arrows point to the end of the abdomen of the specimens. Pictures included under the same ecomorph name represent cases of convergent evolution (i.e., unrelated lineages). (A) *Ctenomorpha marginipennis* (Australia, Lanceocercata) (CC-BY-NC 4.0 Julie Graham, inaturalist.org/observations/73831515); (B) *Phobaeticus kirbyi* (Malaysia, Pharnaciini) (CC-BY-SA 2.0 Bernard Dupont, flickr.com). (C) *Monandroptera acanthomera* (Réunion, Lanceocercata) (© Nicolas Cliquennois, used by permission); (D) *Cranidium gibbosum* (French Guiana, Diapheromerinae) (CC-BY-NC 4.0 Sébastien Sant, inaturalist.org/observations/75953936). (E) *Apterograeffea reunionensis* (Réunion, Lanceocercata) (© Nicolas Cliquennois, used by permission); (F) *Graeffea crouanii* (French Polynesia, Lanceocercata) (CC-BY-NC 4.0 Tahiticrabs, inaturalist.org/observations/165663078). (G) *Leosthenes aquatilis* (New Caledonia, Lanceocercata) (CC-BY-NC 4.0 Damien Brouste, inaturalist.org/observations/24180348); (H) *Pseudoleosthenes irregularis* (Madagascar, African/Malagasy clade) (© Paul Bertner, used by permission). (I) *Epicharmus marchali* (Mauritius, Lanceocercata) (© Sylvain Hugel and Nicolas Cliquennois, used by permission); (J) *Prisopus berosus* (Belize, Pseudophasmatinae) (CC-BY-NC 4.0 Thomas Shahan, inaturalist.org/observations/50919578). (K) *Denhama* sp. (Australia, Lonchodinae) (CC-BY-NC 4.0 Enot Poluskuns, inaturalist.org/observations/166373254); (L) *Clonopsis gallica* (Spain, European clade) (CC-BY 2.0 Ramón Portellano, flickr.com). (M) *Parectatosoma* sp. (Madagascar, African/Malagasy clade) (© Paul Bertner, used by permission); (N) *Taraxippus samarae* (Panama, Cladomorphinae) (© Paul Bertner, used by permission, inaturalist.org/observations/19995010). (O) *Dryococelus australis* (Australia, Lanceocercata) (© Angus McNab, used by permission); (P) *Eurycantha immunis* (Papua, Indonesia, Lonchodinae) (© Chien C. Lee, used by permission). (Q) *Pulchriphyllium bioculatum* (Singapore, Phylliidae) (CC-BY-NC 4.0, Catalina Tong, inaturalist.org/observations/154447000); (R) *Agathemera crassa* (Chile, Pseudophasmatinae) (CC-BY-NC-SA 4.0 Ariel Cabrera Foix, inaturalist.org/observations/29411794).

Phasmatodea (34–38). For example, the “tree lobsters”—flightless, robust, and strongly armored species, including the famous Lord Howe Island stick insect—had been grouped into the subfamily Eurycanthinae but were later shown to be highly polyphyletic, illustrating a dramatic case of morphological convergence (34) (Fig. 1 *O* and *P*). Moreover, several authors have suggested that apterous, stockier, spinier, and darker body forms tend to be found close to the ground, while more elongated and winged forms tend to rest higher up in the vegetation, implicating a role of ecological niche in driving these convergent patterns (32, 39).

We quantitatively assessed the presence and extent of convergent evolution in body morphology in stick insects using a time-calibrated multilocus phylogeny of the order and an associated morphospace of female body morphology. Our analyses identified 21 distinct body types (ecomorphs) and revealed dozens of instances of morphological convergence. These repeated invasions of restricted and distinct portions of the morphospace were associated with behavioral transitions toward similar habitat uses. Using the independent transitions to resting on the leaf litter and trunks ($n = 16$), and to resting on leaves and branches ($n = 16$), we then examined how divergence time, ancestral habitat use, and environmental distance affected the extent of morphological convergence.

Results

Repeated Evolution of Ecomorphs in Phasmatodea. To reconstruct the evolutionary history of Phasmatodea, we used genetic data from three nuclear and four mitochondrial genes across 314 phasmid taxa, and applied Bayesian inferences with six unambiguous crown-group phasmid fossils as minimum calibration points (*SI Appendix, Table S1*). The relationships between the major euphasmatodean clades that arose during an ancient radiation were constrained to match the basal topology inferred in previous phylotranscriptomic studies (36, 40). The inferred Maximum Clade Credibility (MCC) tree was overall strongly supported and was largely congruent with previous studies (Fig. 2 and *SI Appendix, Fig. S1*) (35, 38, 41), providing a robust framework for all subsequent comparative analyses. 16 major clades were recovered and appeared largely defined by geographic distribution and ecozones (Fig. 2 and *SI Appendix, Fig. S1*). The split between Embioptera and Phasmatodea is estimated to have occurred 125 Mya [95% Highest Posterior Density (HPD): 122 to 130 Mya] and between Timematidae and Euphasmatodea to 102 Mya [95% HPD: 99 to 108 Mya].

We assembled a morphological dataset comprising 1,359 adult female specimens from 212 species included in the phylogeny and including 21 quantitative size-controlled measurements (i.e., phylogenetic residuals against body volume) and qualitative data on cuticle texture of the thorax and abdomen (i.e., spiny/rough versus smooth) (*SI Appendix, Fig. S2*). From this dataset, we reconstructed a size-controlled multidimensional morphospace using a mixed Principal Component Analysis (PCAmix) (42). PCAmix combines a PCA with a multiple correspondence analysis, allowing the inclusion of both numerical and categorical variables. This analysis revealed large variation between phasmid species in relative body width (PC1, 50.7% of the total variation), relative wing size (PC2, 11.5%), relative body height (i.e., how flattened the body is; PC3, 9.8%), body texture (i.e., how smooth or rough the body cuticle is; PC4, 7.0%), and relative head size (PC5, 5.3%) (Fig. 3 *A* and *B* and *SI Appendix, Fig. S3*). The first five PCs together accounted for 84.4% of the total variation. The clade Phylliidae (i.e., true leaf insects) stands out from the rest of the phasmids on the morphospace (dark green in Fig. 3 *A* and *B*) as phylliids are characterized by an exceptionally widened and flat

abdomen giving them the appearance of wide angiosperm leaves (Fig. 1 *Q*) (43). Other phasmid clades appeared more centered on the morphospace, varying mostly in relative body width ranging from extremely elongated to more robust body silhouettes (Fig. 3 *A* and *B*). Species with extreme morphologies were scattered at the periphery of this central core, often only projecting out along a single axis. For instance, the large-headed palm stick insects (subfamily Megacraniinae) mostly stand out along the PC5 axis that separates species based on relative head size (Fig. 1 *E* and *F* and *SI Appendix, Table S3*). Most of the morphological diversity is found in the Euphasmatodea, consistent with their much greater species diversity ($n > 3,400$ species), compared to Timematodea ($n = 21$ species), which is morphologically homogeneous (Fig. 3 *C*). The reconstructed morphological diversification of Euphasmatodea can be visualized in *Movie S1*.

We then used an agglomerative hierarchical clustering approach to define and assign species to clusters occupying relatively distinct regions of the multidimensional morphospace (Figs. 3 *A* and *B* and 4 and *SI Appendix, Figs. S4–S6*) (7, 8, 44). The optimum number of clusters ($k = 21$) was determined using the biological homogeneity index [BHI, (45)] to maximize the homogeneity of habitat use within each cluster (*SI Appendix, Fig. S7*). BHI measures the average proportion of taxon pairs with similar habitat uses and which are clustered together morphologically. For 21 clusters, BHI was 0.81, which highlights the strong association between habitat use and the defined morphological clusters, thereafter referred to as ecomorphs following the definition by Williams (i.e., species with a similar habitat, morphology, and behavior, but not necessarily closely related) (46). As expected, among the 21 ecomorphs, we recovered the *wide leaf mimic* ecomorph (only comprising the Phylliidae clade, Fig. 1 *Q*) and the previously recognized *tree lobster* ecomorph (Fig. 1 *O* and *P*), which includes the thorny devil stick insects (*Eurycantha* spp.) and the Lord Howe Island stick insects (*Dryococelus australis*) (34). Using random forest machine learning models (47), we identified the main morphospace axes that were most helpful for these predictive models to infer ecomorph from the morphological data and therefore the axes best distinguishing each ecomorph (*SI Appendix, Table S3*). This analysis revealed that ecomorphs are often distinguished by only a few dimensions of the morphospace. For instance, *spiny robust morphs* were best distinguished by PC1 (i.e., relative body width) and PC4 (i.e., body texture) due to their stocky and rough or spiny bodies, often mimicking bark pieces or moss (Fig. 1 *M* and *N* and *SI Appendix, Fig. S5* and *Table S3*).

A discrete ancestral state reconstruction based on stochastic character mapping (48–50) suggested that the *wide leaf mimic* ecomorph (clade Phylliidae, Fig. 1 *Q*) was the only one with a unique origin (Fig. 3 *C* and *SI Appendix, Table S3*). All other ecomorphs appeared to have originated at least twice (e.g., *Diminutive spiny morph*) and up to at least 10 times (e.g. *broad stick* ecomorph), indicating widespread morphological convergence in the order (Fig. 3 *C*).

Phasmid Morphology and Habitat Use Are Closely Associated. A stochastic character mapping of habitat use reconstructed the ancestor of all phasmatodeans as most likely having rested on the leaf litter, trunks, or logs during the day (Fig. 5 *A*). However, the ancestors of most euphasmatodean clades were inferred as hanging from branches and leaves (Fig. 5 *A*). Overall, this reconstruction indicated between 15 and 19 secondary transitions to resting on the leaf litter, logs, and trunks, 18 transitions to resting on branches and leaves, five to hanging from grass, and two to resting on palm leaves (Fig. 5 *A*). We calculated the size of the multidimensional hypervolumes occupied by each habitat category on the morphospace using range boxes and

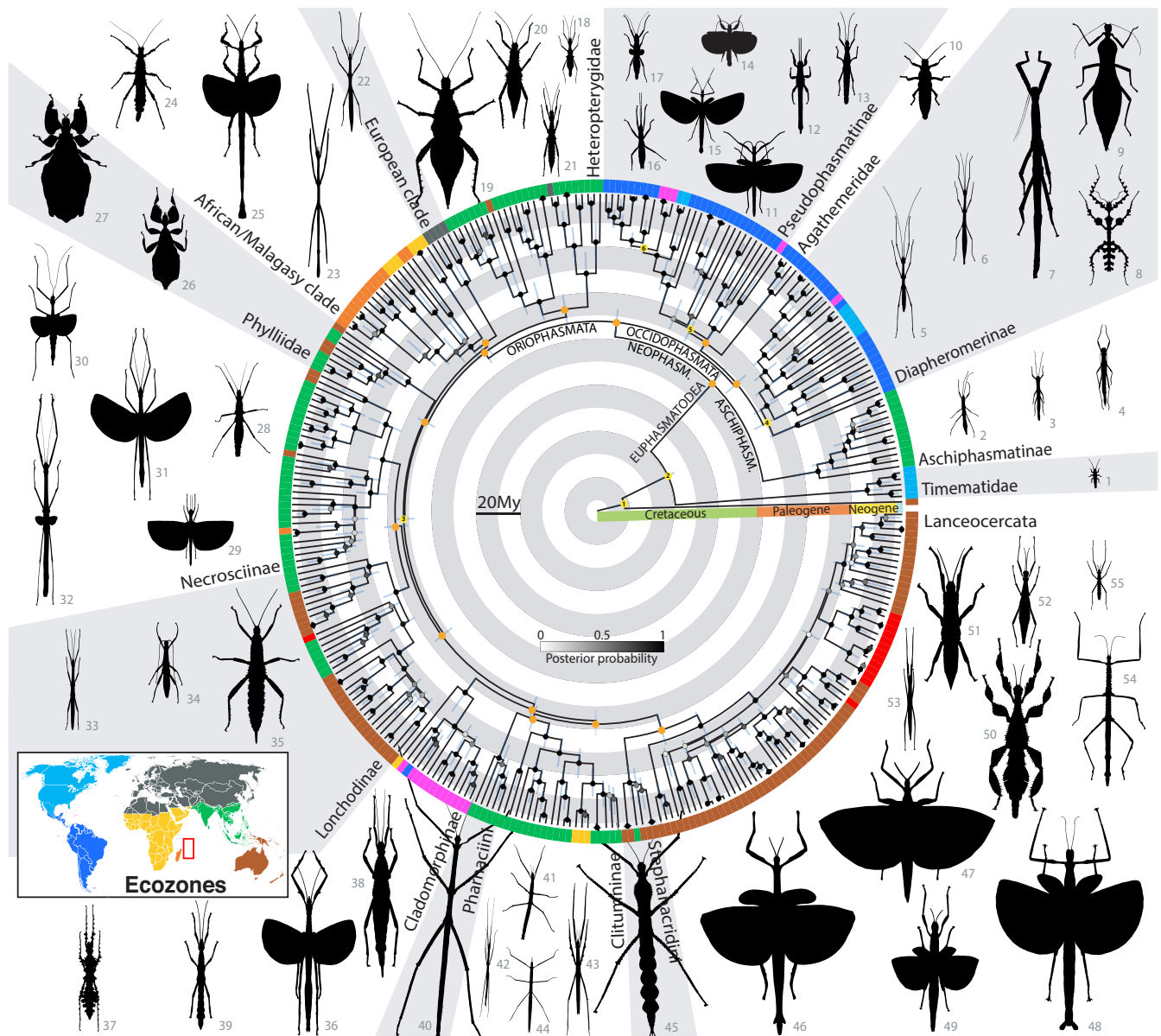


Fig. 2. Time-calibrated MCC tree and geographic distribution of stick and leaf insects. Fossil calibration points are denoted with numbered yellow circles (*SI Appendix, Table S1*). Orange circles correspond to constrained nodes based on the topology inferred from transcriptomes of Tihelka et al. (40). 95% CI around node ages are indicated by blue bars and Bayesian posterior probabilities are indicated by the color of each node (for detailed values see *SI Appendix, Fig. S1*). Tips are colored by eozone following the colors of the map on the bottom left (taxon names are indicated in *SI Appendix, Fig. S1*). The red rectangle on the world map indicates islands of the Mascarene plateau. Scaled adult female silhouettes were drawn by the first author and correspond to the species listed in *SI Appendix, Table S2*.

kernel density estimates (51, 52). Species hanging from branches occupied the largest volume on the morphospace, species hanging from grass or resting on palm leaves the smallest (Fig. 5 *B* and *C* and *SI Appendix, Figs. S8* and *S9*). This reflects the considerable variation in body morphology of species hanging from branches going from extremely elongated and cylindrical stick-like species (e.g., Fig. 1 *A* and *B*) to wide and flat leaf-like species (e.g., Fig. 1 *Q*). Hypervolume overlap, as measured by different methods, was overall relatively low between habitat categories (Jaccard similarity ranged from 0 to 0.17, Sorensen similarity from 0 to 0.29) (*SI Appendix, Figs. S10* and *S11*). Random forest models (i.e., machine learning classification algorithms) reached 84.3% accuracy when classifying the habitat use of taxa based solely on morphospace coordinates (Fig. 5 *D* and *E*). The accuracy of predictions was limited when only based on the first morphospace axis, despite PC1 accounting for more than half of the phenotypic variance (50.7%, *SI Appendix, Fig. S3*), but plateaued

after including the first five axes only (Fig. 5 *E*). Clades varied widely in their occupied hypervolume: Clades displaying diverse habitat uses (e.g., Lanceocercata, African clade) occupied the largest volumes on the morphospace while clades displaying largely uniform habitat uses (e.g., Phylliidae, Heteropterygidae) occupied restricted volumes (Fig. 5 *A* and *SI Appendix, Fig. S12*).

Habitat Transitions Are Associated with Parallel Shifts Toward the Same Morphospacial Regions. We used a series of complementary process- and pattern-based approaches to quantitatively assess the strength of morphological convergence between lineages independently transitioning toward the same habitat use category (hereafter called “convergent lineages”). First, we compared the relative fit of a set of multivariate models of trait evolution [mvMORPH, (53)] and found support for the multiregime Brownian motion model (BMMm), with distinct regimes corresponding to the five

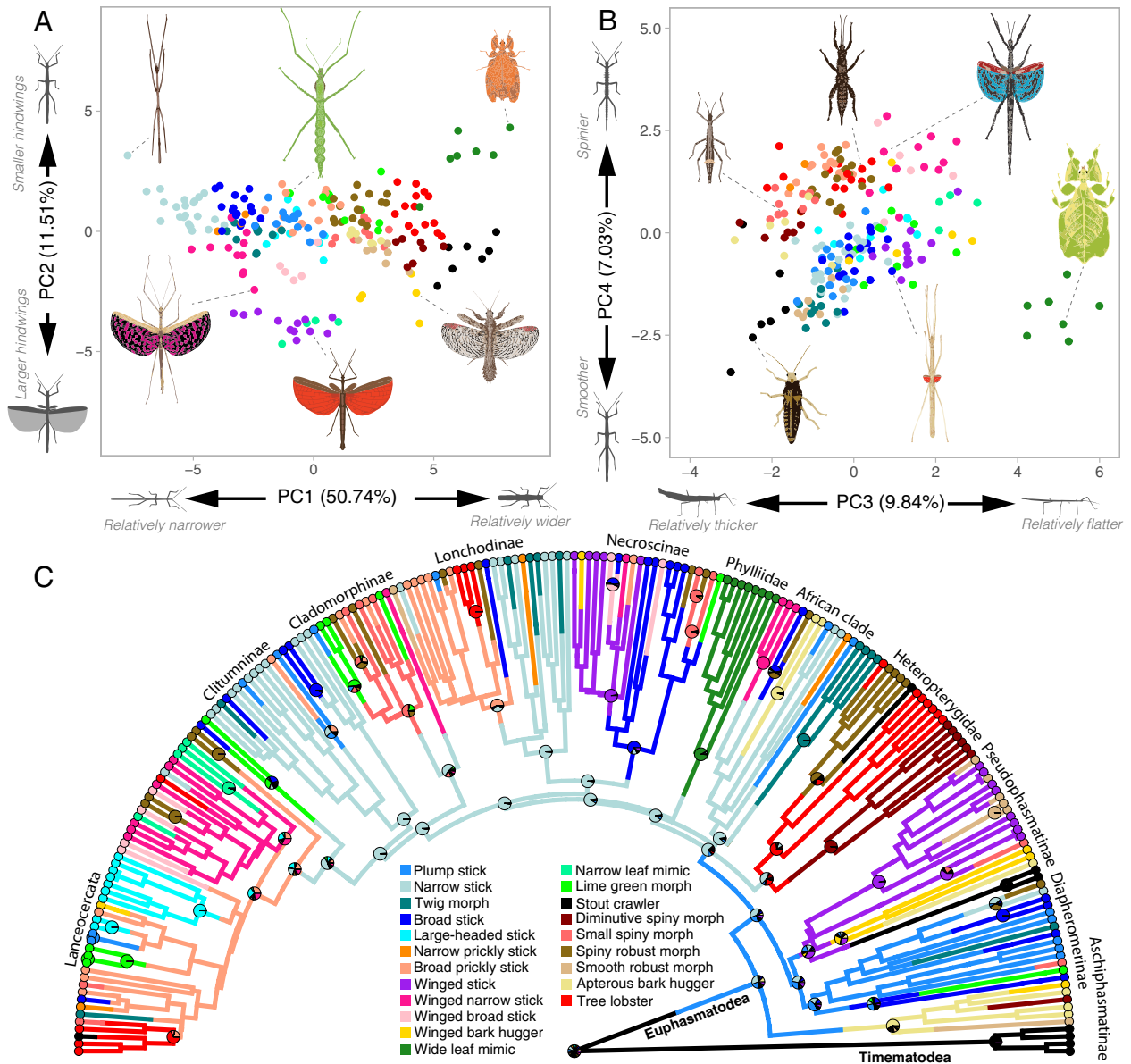


Fig. 3. Repeated ecomorphological evolution in stick and leaf insects. (A and B) Morphospace (first four dimensions) with species colored by assigned ecomorph (Fig. 4). (C) Ancestral state reconstruction of ecomorphs using stochastic character mapping. The pie charts at nodes represent the posterior probabilities that each internal node is in each state. The color legend applies to all panels.

different habitat use categories (i.e., habitat-dependent trait mean and evolutionary rate; *SI Appendix, Table S4*). Thus, habitat use appears to affect morphological evolution but categories did not correspond to unique optima (i.e., specific and restricted morphospacial regions), as BMM models do not model attraction toward optima [in contrast with Ornstein–Uhlenbeck (OU) models, which provided worse fits of our data (*SI Appendix, Table S4*)].

We then assessed the phenotypic similarity between convergent taxa and distinctiveness from other taxa [Wheatshaf index (w), (54, 55)] and the increase in similarity between the convergent taxa through time [C1 to C4 metrics (C-metrics), (10)]. w identified significantly stronger convergence for lineages that independently transitioned to resting on the ground/trunks, to resting on or hanging from branches, and to hanging from grass than would be expected from a random distribution of trait values simulated under a BM model ($P < 0.04$, *SI Appendix, Tables S5 and S6*). Likewise, most of the C1 to C4 statistics were higher than expected under random evolution for all habitats except lineages secondarily transitioning back to hanging from branches (*SI Appendix, Tables S5 and S6*).

The C-metrics rely on the difference between the contemporary distance on the morphospace between two convergent lineages (D_{tip}) and the maximum distance attained between any two points (not necessarily synchronous) along the evolutionary trajectories of the two lineages (D_{max} ; Fig. 6C). Consequently, these metrics can be equally high for lineages that had very dissimilar ancestors at some point in time but then subsequently became more similar, and for lineages shifting in parallel toward a similar region of the morphospace (56). To distinguish between these two scenarios, we computed the recently developed C_t measures, which compare the extant phenotypic distance between the convergent lineages to the maximum reconstructed ancestral distance at a given time point during their evolution (i.e., between synchronous points along the evolutionary trajectories) (56). Unlike C-metrics, C_t -metrics are only expected to be high when lineages diverged morphologically from one another at some point in their evolutionary history and then subsequently got closer (i.e., converged). C_t measures were only significantly higher than expected by chance for transitions to resting on the leaf litter or trunks (*SI Appendix, Tables S5 and S6*).

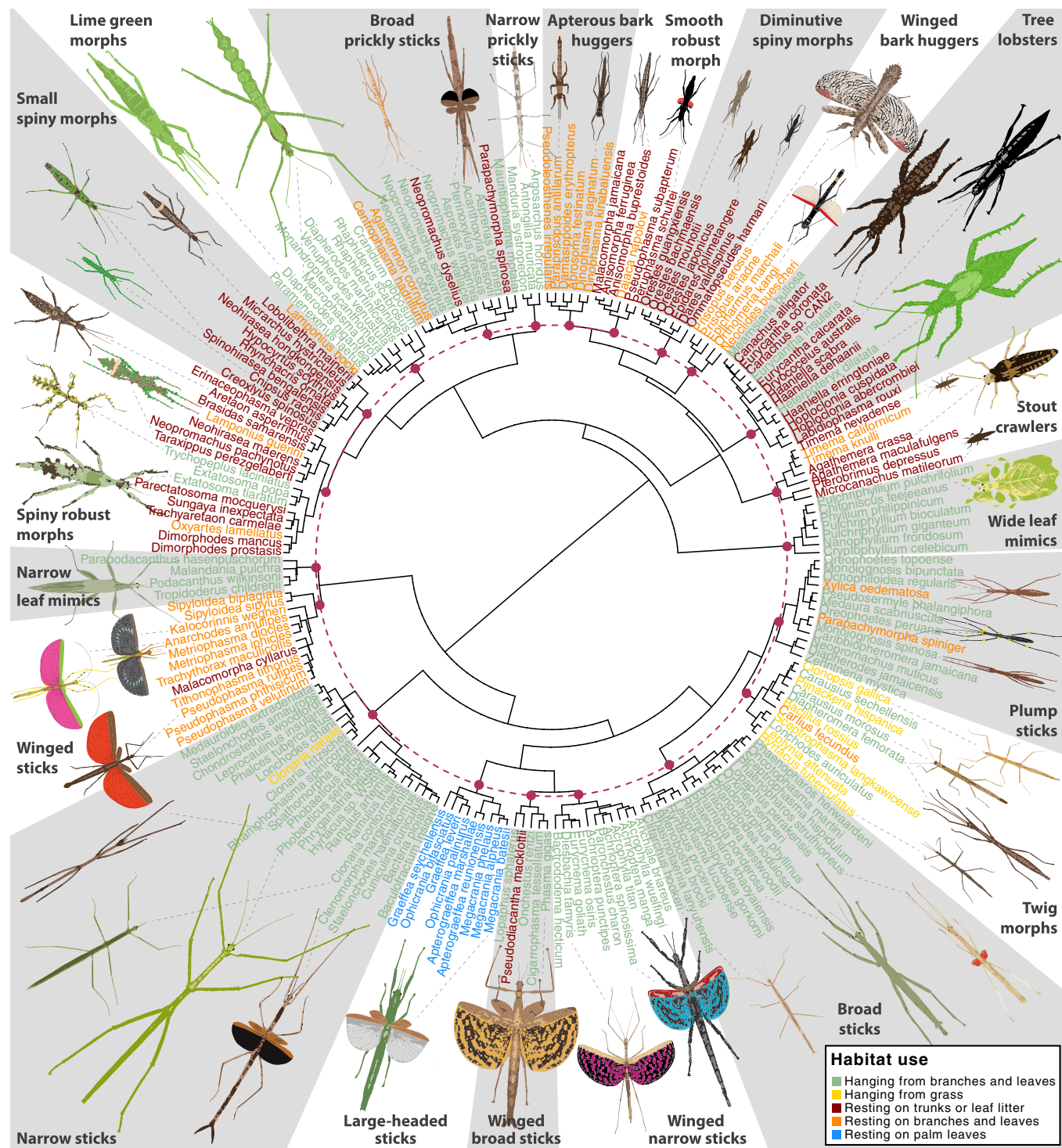


Fig. 4. Phenogram of overall morphological similarity across adult female phasmids. Hierarchical cluster dendrogram based on 21 continuous and two discrete morphological variables using the Ward's method. Tip labels are colored according to extant habitat use. The dashed maroon circle corresponds to the height threshold used to delineate ecomorphs. Intersection between the circle and dendrogram branches is shown as maroon dots. Scaled adult female illustrations correspond to the taxon indicated with a dashed gray line.

But even in this case, C_t values were relatively close to zero, indicating that convergent taxa are not necessarily morphologically closer to one another than their ancestors. This suggests that lineages independently evolving similar habitat uses shifted in parallel toward the same broad region of the morphospace, and sometimes even diverged in that novel region [i.e., “imperfect” convergence (57)] (Fig. 6 A and B). Parallelism [or collinearity (5)] was further confirmed by calculating the pairwise angles between the evolutionary trajectories on the morphospace of convergent lineages

following the independent invasion of a given habitat (θ , Fig. 6C) (27, 58, 59). θ was lower than expected by chance—indicating parallel evolutionary trajectories – for all habitat transitions except one, secondary transitions to hanging from branches (SI Appendix, Tables S5 and S6).

Convergence metrics were generally lower when not controlling for size to build the morphospace (SI Appendix, Table S7), highlighting that convergence in habitat use is mainly associated with convergence in body shape, not size.

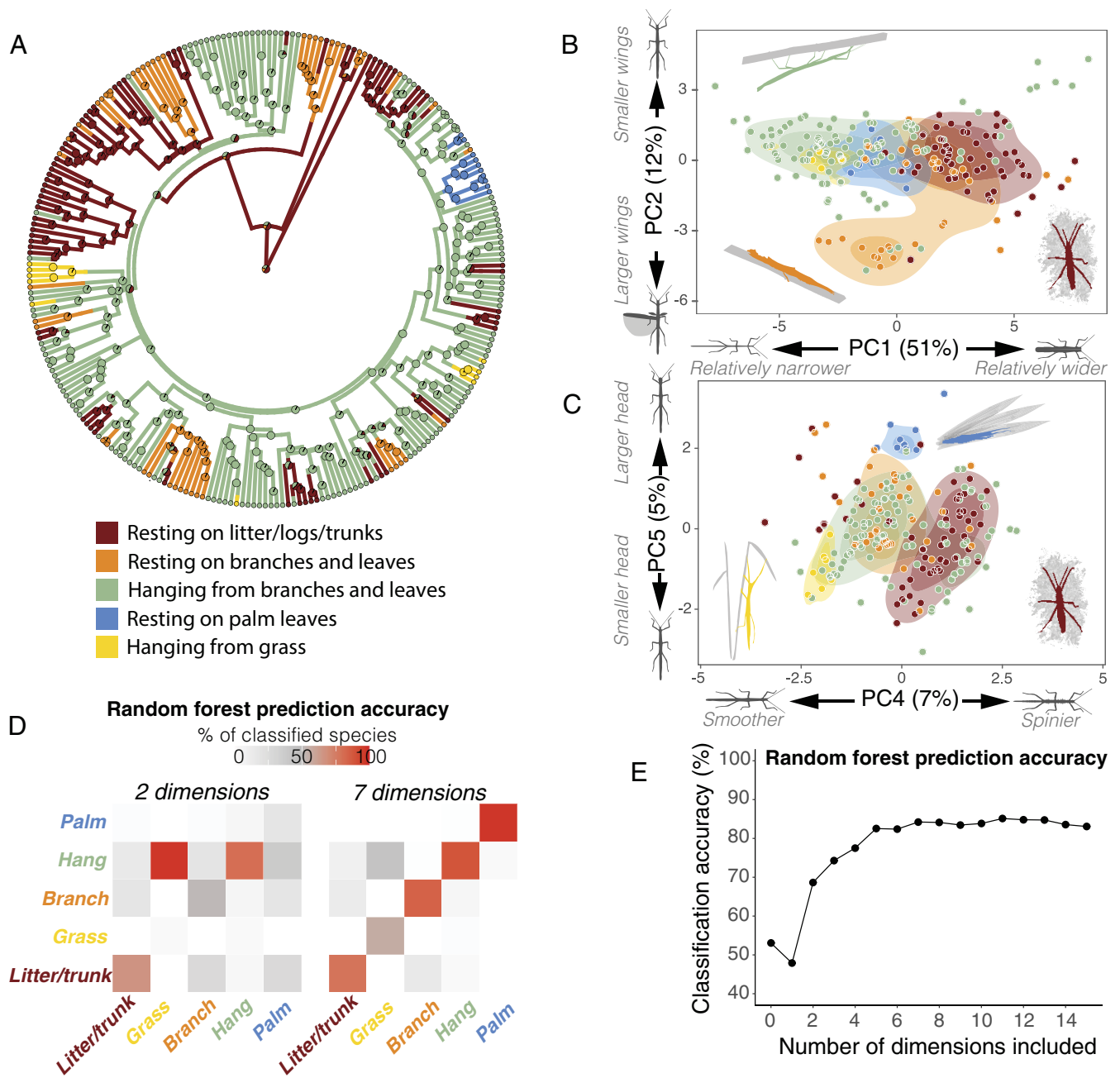


Fig. 5. Habitat transitions and morphospace occupation and overlap between different habitats. (A) Ancestral state reconstruction of habitat use using stochastic character mapping. (B and C) 67% and 33% two-dimensional kernel density contours of species sharing the same habitat on the morphospace (B: PC1 against PC2, C: PC4 against PC5). (D) Heatmaps showing the prediction accuracy of random forest models for each habitat based on two or seven morphospace axes. Predicted habitat states are displayed on the x axis and observed habitat states on the y axis. (E) Mean accuracy of the random forest model at predicting habitat use based on the number of morphospace axes provided.

Environmental Similarity and Phylogenetic Relatedness Promote Stronger Morphological Convergence. Whether two lineages evolve toward close or distant morphospacial regions following a similar habitat use transition may be affected by several factors including whether they started from the same ancestral habitat, the extent of environmental similarities between their new habitats, and their phylogenetic relatedness. We capitalized on the prolific repeated independent habitat transitions in our study (toward resting on the leaf litter and trunks, $n = 16$, Fig. 6A; and toward resting on branches and leaves, $n = 16$, Fig. 6B) to quantify the relative importance of ancestral habitat similarity, environmental distance between derived habitats and time since divergence, on the strength of morphological convergence (the other habitat

transitions were too rare to allow sufficient statistical power [$n \leq 4$, Fig. 5A]). We calculated pairwise environmental distances between convergent lineages as the distance on a multidimensional environmental space built from various macroecological variables relating to habitat height, climatic conditions, plant productivity, and predator diversity (SI Appendix, Fig. S13). For each pair of convergent lineages, we also scored whether they transitioned from the same habitat category or not (binary) and their divergence time as the age of their most recent common ancestor (MRCA). Convergence between pairs of lineages was quantified as pairwise D_{tip} , D_{max} , C_1 , and θ (Fig. 6C).

For both types of habitat use transition, multiple matrix regressions revealed that environmentally closer lineages (i.e., lineages colonizing

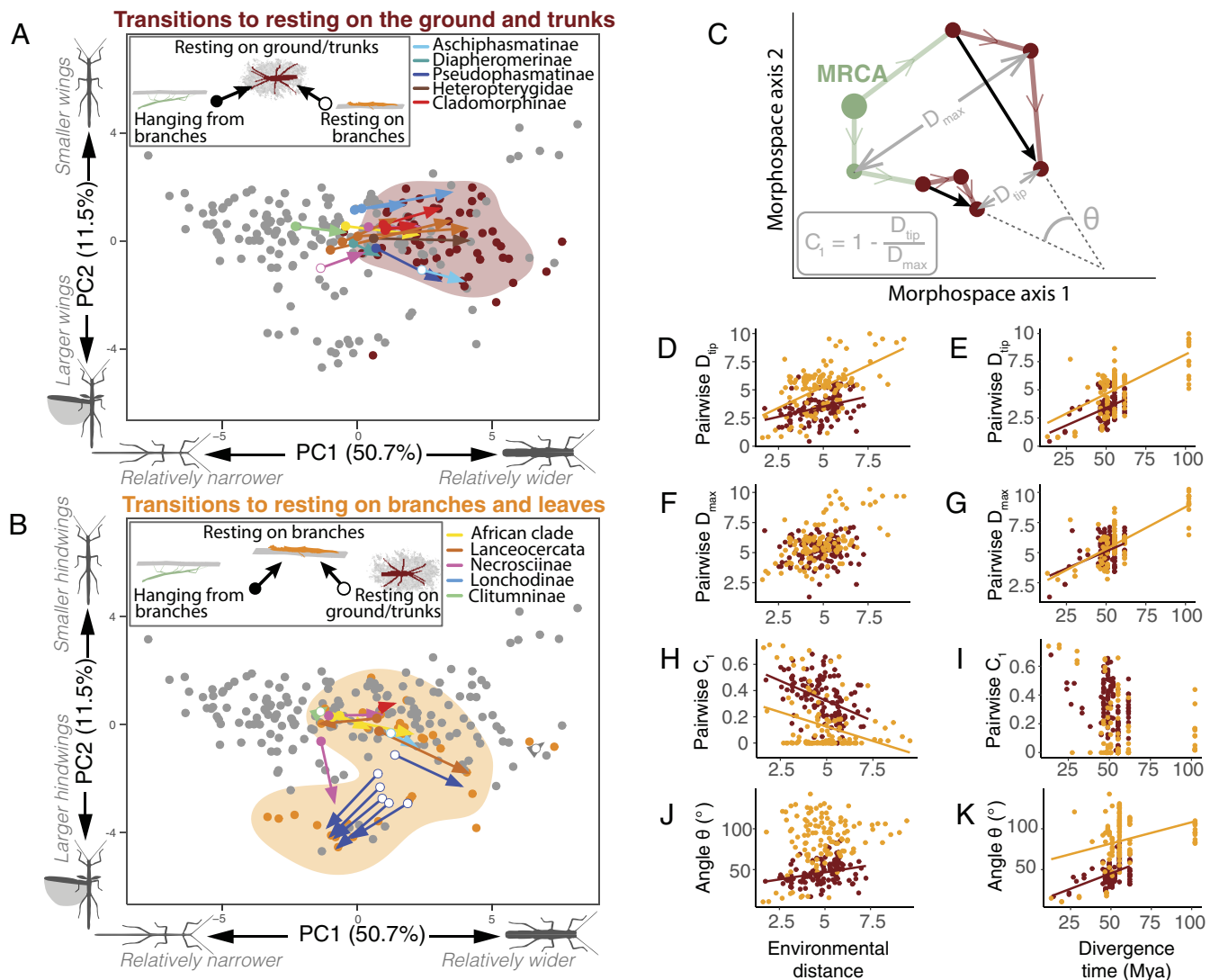


Fig. 6. Evolutionary trajectories and effects of environmental distance and divergence time on morphological convergence. (A and B) Trajectories on the morphospace of lineages that independently transitioned to resting on the ground and trunks (maroon, A) or to resting on branches and leaves (orange, B). Corresponding 75% 2D kernel density contours are shown. Arrows start at the inferred position of the ancestor that first transitioned to the new habitat. Arrows end at the centroid position of descendant species. Arrow colors correspond to genetic clades (Fig. 2). Start symbols indicate the ancestral habitat from which each lineage transitioned according to the *Insets*. (C) Example of the calculation of measures of convergence. The independent trajectories over time of two lineages splitting from their Most Recent Common Ancestor (MRCA) are shown on a morphospace. These lineages start as hanging from branches (pale green) and independently transition to resting on the ground and trunks (maroon). Circles represent ancestral nodes or tips. D_{tip} shows the current morphological distance between the two tips of interest. D_{max} shows the maximum distance between the lineages at any point in time between the tips and the MRCA. C_1 calculates the proportion of the maximum distance between two lineages that has been erased by convergent evolution ($0 \leq C_1 \leq 1$). θ represents the angle between the two vectors starting from the first nodes in the new habitat state and ending at the tips. It compares the overall direction of change between lineages after independently invading the same habitat. (D–K) Pairwise D_{tip} (D and E), pairwise D_{max} (F and G), pairwise C_1 (H and I), and pairwise θ (J and K) as a function of pairwise environmental distance and pairwise divergence time for each independent transition to resting on the ground and trunks (maroon) and resting on branches and leaves (orange). Linear regressions are only shown if the effect of environmental distance and divergence time on the response variable are significant (SI Appendix, Table S8).

more similar selective environments) and more closely related lineages transitioned toward closer positions on the morphospace (i.e., lower D_{tip} ; Fig. 6 D and E and SI Appendix, Table S8). D_{max} was only significantly affected by divergence time between the lineages: Lineages that diverged a long time ago were more likely to exhibit a large D_{max} relative to more closely related ones (Fig. 6 F and G and SI Appendix, Table S8). Consequently, C_1 decreased with environmental distance indicating weaker convergence between lineages experiencing more dissimilar environmental conditions (Fig. 6 H and SI Appendix, Table S8), and was only weakly affected by divergence time (Fig. 6 I and SI Appendix, Table S8). θ was primarily affected by divergence time: More closely related species pairs tended to follow more parallel evolutionary trajectories (Fig. 6 J–K and SI Appendix, Table S8). Lineages that transitioned toward the same habitat use category from different ancestral categories and thus potentially starting from further

apart on the morphospace exhibited less parallel trajectories. However, this effect was only significant for the repeated transitions to resting on branches and leaves (SI Appendix, Table S8). These patterns were largely similar when using coordinates from a PCA controlling for phylogenetic covariance but excluding the two categorical variables on body texture (SI Appendix, Table S9). However, they were not recovered when using coordinates from a PCA not controlling for size (SI Appendix, Table S10) as habitat use appears to mainly drive convergence in body shape but not in body size.

Discussion

When adapting to shared environmental challenges, lineages often vary in the extent to which they evolve similar traits, indicating that evolutionary outcomes are more predictable in some instances

than in others. Explaining this variation will be critical as scientists increasingly base medical (vaccine design, pandemic preparedness, antibiotic resistance, cancer therapies), agricultural (application of herbicides and pesticides, anticipating crop responses to climate change), and conservation (wildlife responses to anthropogenic disturbance and climate change) practices on predicted evolutionary responses to selection (60, 61). Here, we used the dozens of instances of repeated habitat use transition in stick and leaf insects to quantify the relative contributions of divergence time (phylogenetic relatedness), similarity of most recent ancestral habitat, and the similarity of invaded environments, to the repeatability—and therefore the predictability—of phenotypic evolution. As in earlier studies of repeated evolution, we show that closely related lineages (i.e., likely sharing more genetic variation) followed more parallel evolutionary trajectories and ended up relatively closer on the morphospace, consistent with the idea that in the absence of opportunity for contingency, phenotypic responses to selection will be highly predictable (27, 62). Our study encompassed a wide range of divergence times (10 to 100 My) and a large number of repeated habitat use transitions, permitting us to also show that the strength of morphological convergence decreases steadily with time since divergence (Fig. 6 D–K and *SI Appendix, Table S8*). Ironically, this suggests that for morphological evolution even the stochastic contributions of contingency are predictable, in the sense that they accrue at a rather constant rate over time.

Classic examples of morphological convergence are often found among closely related taxa [e.g., *Anolis* lizards (15, 16), stickleback fish (17), cichlid fish (44)], suggesting that the repeatability of phenotypic evolution increases with relatedness (11). Closely related lineages appear predisposed to adapt in more similar ways when confronted with similar challenges, consistent with Gould's idea that evolution is less inclined to repeat itself at large macroevolutionary time scales (18). Here, we provide an original and direct test of this idea in a system spanning vast divergence times (10 to 100 My) (36, 40). In phasmids Gould's pattern was manifest in two ways: More closely related lineages responding independently to similar environmental challenges ended up looking more similar (i.e., more extensive convergence), and they followed more parallel paths on the morphospace to arrive there, than more distantly related lineage pairs. Closely related lineages likely share more standing genetic variation, and segregating variants are expressed against more similar genetic backgrounds (22, 63–65); and they are more likely to reuse the same genes when they adapt to similar environmental challenges (23–26).

The other factor influencing the strength of convergence is the environment: The more similar the selective conditions experienced by two lineages, the closer the resulting convergent phenotypes. Studies of phenotypic convergence often categorize ecological niches to identify associations between patterns of morphological evolution and the repeated adaptation to these discrete niches [e.g., diet types (57), lakes/streams (7, 12)]. This categorization hides potential heterogeneities in environmental conditions among instances of the same category. Conditions that appear similar to a human observer may actually be disparate to the organisms, and this can confound studies attempting to explain variation in the strength of convergence. For example, stickleback fish independently colonizing stream habitats varied in the extent of their phenotypic convergence in part because habitats categorized as “stream” actually differed in water clarity, temperature, parasite abundance, and food availability (27). Once these additional variables had been included, habitat similarity predicted the resulting strength of convergence more accurately (27).

Here we quantified niche similarity using various macroecological variables, and our results suggest that some of the niches

invaded by phasmids (e.g., grass) were largely uniform and thus likely experienced very similarly across lineages, while others (e.g., resting on branches and leaves) encompassed much wider and potentially less similar environmental conditions (i.e., they likely included “cryptic” dissimilarities between habitat use categories) (*SI Appendix, Fig. S14*). We show that environmental similarity of invaded habitats also predicted strength of convergence: Lineages switching to more similar environments within a given habitat use category ended up in closer regions of the morphospace (Fig. 6 D and H), even across large macroevolutionary time scales and despite the higher associated opportunities for contingency.

Finally, we accounted for similarity of the most recent *ancestral* habitats of convergent pairs of lineages, to test whether transitioning from the same or different habitat categories affected the extent of the resulting convergence in this group of insects. Lineages that transitioned toward the same habitat *from the same ancestral habitat* tended to follow more parallel or collinear trajectories, but this effect was only significant for transitions to resting on branches and leaves (*SI Appendix, Table S8*). It is possible that there were not enough transitions from the same versus different ancestral habitats for transitions to resting on trunks and leaf litter to detect this effect.

The Euphasmatodea show a deep radiation at the base of the group (~65 to 55 Mya) following the K-T boundary (36), corresponding with the origin of most major clades and with dispersal across vast regions of the globe (Fig. 2 and *SI Appendix, Fig. S1*). Although a few of these clades seem to have undergone speciation without niche differentiation, and species within these clades are morphologically homogeneous [e.g., Phylliidae (wide leaf mimics and canopy-dwellers) and the Heteropterygidae (spiny and robust ground-dwellers), which are distributed on many islands of Indomalaya and Australasia (Figs. 3C and 4A and *SI Appendix, Fig. S12*) (43, 66)], the majority of euphasmatodean clades subsequently radiated into multiple different ecomorphs colonizing diverse habitats [e.g., Lanceocercata (Australasia and Mascarene islands), Cladomorphinae (Caribbean islands), Lonchodinae (Indomalaya/Australasia), Necrosciinae (Indomalaya), African/Malagasy clade (Afrotropics), Pseudophasmatinae (Nearctic and Neotropics), and Diapheromerinae (Nearctic and Neotropics); Figs. 3C and 5A and *SI Appendix, Fig. S12*) (34, 43, 66, 67)]. We characterized 21 different phasmid ecomorphs and reconstructed dozens of evolutionary transitions between ecological niches, resulting in repeated instances of convergence toward these phasmid body forms. Overall, our results suggest the extremely diverse morphologies of stick and leaf insects result from replicated radiations in different geographic regions, each associated with widespread parallel shifts on the morphospace as independent lineages adapted to similar habitats.

Conclusion

Stick and leaf insects exemplify the extraordinary power of natural selection to shape organismal phenotypes. The animals themselves are charismatic champions of crypsis and masquerade, and our comprehensive quantification of their trajectories of morphological evolution, using process-based (i.e., evolutionary modeling) and pattern-based methods, reveals dozens of instances of convergence. We show that the details of the environmental conditions experienced by the organisms—the closeness of the invaded niches and the similarity of their starting, or ancestral, niche—predict the extent of convergence even when the lineages in question have been evolving independently for tens of millions of years, and therefore have had ample opportunity for contingency. Furthermore, we show that even the effects of contingency are predictable, eroding the strength of convergence at a gradual and steady rate across vast spans

of time. We suggest that precise quantification of selective environments, as well as divergence times, will be critical as studies increasingly attempt to predict the outcomes of evolution.

Materials and Methods

Extended materials and methods are reported in *SI Appendix, Supplementary Materials and Methods*, and include details on definitions and choices of convergence metrics.

Taxonomic Sampling and Phylogenetic Reconstruction. Well-supported phylogenies for 38 phasmid lineages representing all major clades of Phasmatodea were recently reconstructed using next-generation sequencing (transcriptomes), yielding topologies that resolved most of the deep nodes within this group with high confidence (36, 40). Here we reconstructed a phylogeny with 314 species representing all major phasmid lineages (9% of the known phasmid species diversity and 33% of currently recognized generic diversity), and one species of Embioptera (the sister clade of Phasmatodea) as outgroup, constraining the basal topology to match the transcriptome-based trees (40). Regions of three nuclear [18S rRNA (18S), 28S rRNA (28S), and histone subunit 3 (H3)] and four mitochondrial genes [12S rRNA (12S), 16S rRNA (16S), cytochrome-c oxidase subunit I (COI) and COII] were extracted from Genbank, aligned and concatenated (6,778 bp total) to reconstruct a MCC tree for phasmids using Bayesian inferences in BEAST 2 (v. 2.6.3) (*Dataset S1*) (68). Divergence time was estimated using six unambiguous crown-group phasmid fossils as minimum calibration points (*SI Appendix, Table S1*).

Morphological Data. We examined 1,359 adult female specimens from 212 species included in the phylogeny. High-quality photographs, captured in dorsal and/or lateral views, were obtained from our own collection at the University of Göttingen (Germany), other museum collections, the published literature, and other online sources (*Dataset S1*). Depending on material availability, we measured pictures of between 1 and 18 different individuals per species (mean = 5.5 individuals per species). We collected 21 continuous measurements (*SI Appendix, Fig. S2*) that together contained biologically relevant information about overall body size and shape, width, and length of different body segments (notably the head), leg length, hindwing size, and the length of the subgenital plate (whose function is often related to oviposition). We also qualitatively scored the texture of the mesothorax and abdomen (1: spiny/rough, 0: smooth). Body volume was used as a proxy for body size and was calculated as the volume of an elliptical cylinder of the same length, average width, and height as the body of the insect (*SI Appendix, Fig. S2*).

The Phasmid Morphospace. We built a multidimensional morphospace using a PCA mixing continuous and categorical data (PCA_{mix}) (42). To avoid differences in body size (which can vary by as much as 300-fold in volume) dominating differences in body shape and to remove allometric effects, we size-corrected the continuous measurements (6, 12, 69). We substituted original measurement values with the residuals calculated from a phylogenetically corrected linear regression against body volume (R package “phytools”) (50, 70), after \log_{10} -transformation. Because wing length and wing area included zeros for wingless species, we divided the non-transformed measurements by body length or body length squared respectively, to obtain and include measures of relative wing length and area. In total, we included 21 continuous (previously mean-centered on zero and scaled to unit variance) and two categorical variables (*SI Appendix, Figs. S2 and S3*). To make sure that categorical variables and size correction were not biasing our results, we also ran PCAs including a phylogenetic correction and excluding the two categorical variables. The continuous variables were either corrected for size ($pPCA_c$) or not ($pPCA_{nc}$) (*SI Appendix, Figs. S15 and S16 and Supplementary Materials and Methods*).

Habitat Data. We broadly classified the habitat use of stick insects based on the typical resting posture and substrate preferences exhibited by adult females when hiding during the day (i.e., when they are exposed to visually hunting predators). We surveyed the literature, field guides, and iNaturalist (<https://www.inaturalist.org/>, accessed July 2021) for observations of where each species is typically found (*Dataset S1*). We defined five habitat use categories: resting on the ground or trunks (including the base of trunks, mossy logs, under bark, in the leaf litter), resting on branches and leaves, hanging from branches and leaves, hanging from grass, and resting on palm leaves. We acknowledge that this classification is broad

and consequently does not fully encompass the entire spectrum of substrates and host plants upon which phasmids may be found (31–33).

Environmental Data. We gathered information about the geographic range of each species based on sampling location of type specimens and observations on iNaturalist (available from <https://www.inaturalist.org>, accessed July 2021). For each species, we then selected the median location with the most central latitude. From the GPS coordinates of the most central location for each species, we extracted data on 17 environmental variables that together contained information about climatic conditions (temperature, precipitation, seasonality), vegetation density and food availability (primary production), predator diversity, and habitat vegetation layer (*Dataset S1*). Variation in these variables was summarized by running a PCA (*SI Appendix, Fig. S13*).

Definition of Ecomorphs. We used our multidimensional morphospace data (PCA_{mix}) to cluster species into distinct ecomorphs by running a hierarchical clustering algorithm (using the Ward’s method) to define ecomorphs based on overall proximity on the morphospace (defined by the first seven PC axes, accounting for 90% of the total variation). We defined the optimal number of clusters using the BHI, which measured how homogeneous clusters are, based on habitat use (R package “cValid”) (45, 71). Clusters were defined by a fixed height threshold on the clustering dendrogram. The optimal number of clusters was then chosen to minimize the number of clusters while maximizing BHI (i.e., start of a plateau, *SI Appendix, Fig. S7*). We then identified the morphospace axes that best distinguished each ecomorph by training random forest models (R package “randomForest”) (47) to classify a taxon in either an ecomorph of interest or in a different one, given the first seven axes of the PCA_{mix} morphospace (*SI Appendix, Table S3*).

Overlap between Habitat Categories on the Morphospace. To quantify morphospace occupation by species exhibiting different habitat uses (Fig. 5 B and C), we estimated multidimensional hypervolumes using dynamic range boxes (R package “dynRB”) (51) and high-dimensional kernel density estimations (R package “hypervolume”) (52), including either PC1 to PC7 of PCA_{mix} (90.1% of the total variation), PC1 to PC8 of $pPCA_{nc}$ (91.5%), or PC1 to PC6 of $pPCA_c$ (92.1%) (*SI Appendix, Figs. S8 and S9*). Pairwise hypervolume overlap was quantified for the PCA_{mix} morphospace as the portion of the hypervolume of habitat A covered by the hypervolume of habitat B and vice versa, as the Jaccard similarity index (ratio of the intersection to the union of the hypervolumes), or as the Sørensen-Dice similarity index (ratio of twice the size of the intersection to the sum of the individual hypervolumes) (*SI Appendix, Figs. S10 and S11*). The distance between the hypervolumes was also quantified as the Euclidean distance between the hypervolume centroids and the minimum Euclidean distance between points of the two hypervolumes (*SI Appendix, Fig. S11*). Finally, we also quantified the overlap between the habitat categories on the PCA_{mix} morphospace using machine learning random forest models (47). These models were used to predict the habitat category of a species given its position on the morphospace. The predictive error rate of the models was used to quantify overlap between habitat categories (Fig. 5 D and E).

Ancestral State Reconstruction of Ecomorphs and Habitat Use. Habitat use was mapped on the MCC tree to uncover the number of independent transitions toward each of the five categories (Fig. 5A). We ran ancestral state reconstructions using stochastic character mapping as implemented in the R package “phytools” (50). The transition matrix was calculated using maximum likelihood and using an all-rates-different model (model = “ARD”). Ecomorphs, as defined by our hierarchical clustering analysis, were similarly mapped to establish whether they had single or multiple origins (Fig. 3C). Given the large number of ecomorphs ($n = 21$), only the “equal rate” transition model (assuming a single transition rate between ecomorphs) could be run.

Process-Based Tests of Convergence—Evolutionary Model Fitting. To test for morphological convergence among lineages that independently transitioned to the same habitat, we fitted multivariate models of continuous trait evolution to PC1 to PC5 (PCA_{mix} , 84% of the total variance) using the “mvMORPH” R package (53). We first fit the single-regime Brownian motion (BM1, modeling stochastic trait changes over time), Ornstein-Uhlenbeck (OU1, modeling attraction toward an optimal trait value), and early burst models (EB, modeling stochastic changes with a decrease in evolutionary rate over time), which represent the null

hypotheses. Then, for each habitat category, we fit two-regime models where the given habitat category was considered its own evolutionary regime while the rest belonged to another unique regime. We also ran five-regime models including each habitat as a separate regime. The ancestral histories for each of the tested regime assignments were reconstructed on the MCC tree using 100 stochastic character maps (50). We fitted multiregime OU models allowing trait optima to vary among regimes, and BM models allowing on one hand the phylogenetic means to vary among regimes, and on the other hand holding the evolutionary rate constant (BM1m) or not (BMMm).

Pattern-Based Tests of Convergence. To quantify the strength of morphological convergence associated with repeated habitat transitions, we calculated the C1 to C4 pattern-based metrics (R package “convevol”) (10) as well as the Wheatseaf index (w) (“windex”) (54, 55) for PC1 to PC7 of PCA_{mix} (90.1% of the total variation), PC1 to PC8 of pPCA_{nc} (91.5%), and PC1 to PC6 of pPCA_c (92.1%). C₁–C₄ are based on the ratio between the current distance between two lineages (D_{tip}) on the morphospace to the maximum reconstructed distance between the two lineages at any point in the past (D_{max}) (Fig. 6C). C₁–C₄ will be high when independent lineages diverged substantially after splitting and then subsequently re-evolved similarities, or when convergent lineages shifted in parallel toward the same direction on the morphospace (56). To distinguish between these two scenarios, we computed the recently developed Ct₁–Ct₄ metrics, which restrict D_{max} to synchronous nodes (56). Ct₁–Ct₄ are only expected to be high in the first scenario (divergence first, then convergence). Finally, we quantified parallelism in the evolutionary trajectories of convergent lineages by calculating the angle (θ) between these trajectories on the morphospace (58, 59, 72). We reconstructed the trajectories of convergent lineages from the position of the node immediately prior to the inferred habitat transition, to that of the tip of interest (Fig. 6C). For each above-described variable, P -values were inferred following 1,000 simulations of random character evolution, testing the hypothesis that convergence is significantly stronger (or that trajectories are more parallel) in the habitat category of interest than would be expected by chance.

Explaining Variation in the Extent of Morphological Convergence. We tested the effects of three factors on the extent of morphological convergence: the phylogenetic relatedness between the convergent lineages, their environmental similarity, and whether they started from the same ancestral habitat use category. We only considered the repeated transitions toward resting on the leaf litter and trunks ($n = 16$, Fig. 6A) and toward resting on branches and leaves ($n = 16$, Fig. 6B) for these analyses as other transitions were too rare to allow sufficient statistical power ($n \leq 4$, Fig. 5A). For each transition type, phylogenetic relatedness, environmental distance, ancestral habitat difference, and morphological convergence were computed for all possible pairs of taxa corresponding to separate independent transitions toward the habitat category, and then assembled

as distance matrices. Pairwise phylogenetic relatedness was estimated as the age of the MRCA of the two lineages. Pairwise environmental distance was calculated as the Euclidean distance on the environmental PC1 to PC7 (accounting for 90% of the total environmental variation). Pairwise ancestral habitat difference was scored as either 0 if both lineages transitioned to the habitat of interest from the same ancestral habitat, or 1 otherwise. Finally, to quantify morphological convergence, we computed pairwise D_{tip} , pairwise D_{max} , pairwise C₁, and pairwise θ using PC1 to PC7 of PCA_{mix} (90.1% of the total variation), PC1 to PC8 of pPCA_{nc} (91.5%), or PC1 to PC6 of pPCA_c (92.1%). We fitted multiple matrix regressions (partial Mantel tests, R package “phytools”) with 100,000 Mantel permutations to compute P -values. Phylogenetic relatedness, environmental distance, and ancestral habitat difference were included as explanatory variables, and either D_{tip} , D_{max} , C₁, or θ as response variables. The choice of variables to compare the magnitude of convergence across independent habitat transitions is extensively discussed in supplementary information. Finally, we verified the robustness of the recovered patterns to the independent habitat transitions we included by bootstrap sampling the two types of independent transitions 100 times, and checking the consistency of the effects of the three explanatory variables on the different response variables.

Data, Materials, and Software Availability. All data and code used in this study have been deposited and made publically available at Zenodo (10.5281/zenodo.13774069) (73). All other data are included in the article and/or supporting information.

ACKNOWLEDGMENTS. We thank Camille Thomas-Bulle, Tanja Schwander, Anthony Lapsansky, Guillaume Lavanchy, and William Toubiana for insightful discussions on the manuscript. This study would not have been possible without the work of many passionate phasmid enthusiasts and breeders who, over the years, documented the biology of many species. We are therefore very grateful to the amateur and professional phasmid community for publicly or privately sharing these notes and observations along with many high-quality pictures. We are thankful to Nicolas Cliquennois for insightful discussions regarding Malagasy and Mascarene stick insects. We thank Paul Bertner, Angus McNab, Chien C. Lee, Bruno Kneubühler, Nicolas Cliquennois, and Paul Brock for permission to use their pictures. Finally, we thank Jonathan B. Losos and Scott V. Edwards for reviews that substantially improved this manuscript. This research was supported by NSF IOS-2015907 to D.J.E.

Author affiliations: ^aDivision of Biological Sciences, University of Montana, Missoula, MT 59812; ^bDepartment of Ecology and Evolution, University of Lausanne, Lausanne CH-1015, Switzerland; and ^cDepartment of Animal Evolution and Biodiversity, Johann-Friedrich-Blumenbach Institute of Zoology and Anthropology, University of Göttingen, Göttingen D-37073, Germany

1. S. Conway Morris, *The Runes of Evolution: How the Universe Became Self-Aware* (Templeton Press, 2015).
2. G. R. McGhee, *Convergent Evolution: Limited Forms Most Beautiful* (MIT Press, 2011).
3. J. B. Losos, Convergence, adaptation, and constraint. *Evolution* **65**, 1827–1840 (2011).
4. D. B. Wake, M. H. Wake, C. D. Specht, Homoplasy: From detecting pattern to determining process and mechanism of evolution. *Science* **331**, 1032–1035 (2011).
5. J. Cerca, Understanding natural selection and similarity: Convergent, parallel and repeated evolution. *Mol. Ecol.* **32**, 5451–5462 (2023).
6. D. M. Grossnickle *et al.*, Incomplete convergence of gliding mammal skeletons. *Evolution* **74**, 2662–2680 (2020).
7. P. Trontelj, A. Blejec, C. Fišer, Ecomorphological convergence of cave communities. *Evolution* **66**, 3852–3865 (2012).
8. Š. Borko, P. Trontelj, O. Seehausen, A. Moškrič, C. Fišer, A subterranean adaptive radiation of amphipods in Europe. *Nat. Commun.* **12**, 1–12 (2021).
9. R. G. Gillespie, S. P. Benjamin, M. S. Brewer, M. A. J. Rivera, G. K. Roderick, Repeated diversification of ecomorphs in Hawaiian stick spiders. *Curr. Biol.* **28**, 941–947 (2018).
10. C. T. Stayton, The definition, recognition, and interpretation of convergent evolution, and two new measures for quantifying and assessing the significance of convergence. *Evolution* **69**, 2140–2153 (2015).
11. T. J. Ord, T. C. Summers, Repeated evolution and the impact of evolutionary history on adaptation. *BMC Evol. Biol.* **15**, 1–12 (2015).
12. D. Esquerré, J. Scott Keogh, Parallel selective pressures drive convergent diversification of phenotypes in pythons and boas. *Ecol. Lett.* **19**, 800–809 (2016).
13. Z. D. Blount, R. E. Lenski, J. B. Losos, Contingency and determinism in evolution: Replaying life's tape. *Science* **362**, eaam5979 (2018).
14. A. A. Agrawal, Toward a predictive framework for convergent evolution: Integrating natural history, genetic mechanisms, and consequences for the diversity of life. *Am. Nat.* **190**, S1–S12 (2017).
15. J. B. Losos, T. R. Jackman, A. Larson, K. De Queiroz, L. Rodríguez-Schettino, Contingency and determinism in replicated adaptive radiations of island lizards. *Science* **279**, 2115–2118 (1998).
16. L. D. Mahler, T. Ingram, L. J. Revell, J. B. Losos, Exceptional convergence on the macroevolutionary landscape in island lizard radiations. *Science* **341**, 292–295 (2013).
17. P. F. Colosimo *et al.*, Widespread parallel evolution in sticklebacks by repeated fixation of ectodysplasin alleles. *Science* **307**, 1928–1933 (2005).
18. S. J. Gould, *Wonderful Life: The Burgess Shale and the Nature of History* (W. W. Norton & Company, 1989).
19. S. J. Gould, *The Structure of Evolutionary Theory* (Harvard University Press, 2002).
20. V. Orgogozo, Replaying the tape of life in the twenty-first century. *Interface Focus* **5**, 20150057 (2015).
21. R. D. H. Barrett, S. M. Rogers, D. Schluter, Natural selection on a major armor gene in threespine stickleback. *Science* **322**, 255–257 (2008).
22. G. L. Conte, M. E. Arnegard, C. L. Peichel, D. Schluter, The probability of genetic parallelism and convergence in natural populations. *Proc. R. Soc. B* **279**, 5039–5047 (2012).
23. M. Bohutínská *et al.*, Genomic basis of parallel adaptation varies with divergence in Arabidopsis and its relatives. *Proc. Natl. Acad. Sci. U.S.A.* **118**, e2022713118 (2021).
24. S. Chaturvedi *et al.*, Climatic similarity and genomic background shape the extent of parallel adaptation in Timema stick insects. *Nat. Ecol. Evol.* **6**, 1952–1964 (2022).
25. G. Montejo-Kovacevich *et al.*, Repeated genetic adaptation to altitude in two tropical butterflies. *Nat. Commun.* **13**, 1–16 (2022).
26. I. S. Magalhaes *et al.*, Intercontinental genomic parallelism in multiple three-spined stickleback adaptive radiations. *Nat. Ecol. Evol.* **5**, 251–261 (2021).
27. Y. E. Stuart *et al.*, Contrasting effects of environment and genetics generate a continuum of parallel evolution. *Nat. Ecol. Evol.* **1**, 1–7 (2017).
28. M. Bohutínská, C. L. Peichel, Divergence time shapes gene reuse during repeated adaptation. *Trends Ecol. Evol.* **39**, 396–407 (2024).
29. G. D. Ruxton, W. L. Allen, T. N. Sherratt, M. P. Speed, *Avoiding Attack: The Evolutionary Ecology of Crypsis, Aposematism, and Mimicry* (Oxford University Press, 2019).
30. J. Skelhorn, H. M. Rowland, M. P. Speed, G. D. Ruxton, Masquerade: Camouflage without crypsis. *Science* **327**, 51 (2010).

31. G. O. Bedford, Biology and ecology of the Phasmatodea. *Annu. Rev. Entomol.* **23**, 125–149 (1978).
32. S. Bradler, T. R. Buckley, "Biodiversity of Phasmatodea" in *Insect Biodiversity: Science and Society*, R. G. Footitt, P. H. Adler, Eds. (Wiley-Blackwell, 2018), pp. 281–313.
33. P. D. Brock, T. H. Büscher, *Stick and Leaf-Insects of the World* (NAP Editions, 2022).
34. T. R. Buckley, D. Attanayake, S. Bradler, Extreme convergence in stick insect evolution: Phylogenetic placement of the Lord Howe Island tree lobster. *Proc. R. Soc. B* **276**, 1055–1062 (2009).
35. S. Bradler, N. Cliquennois, T. R. Buckley, Single origin of the Mascarene stick insects: Ancient radiation on sunken islands? *BMC Evol. Biol.* **15**, 1–10 (2015).
36. S. Simon *et al.*, Old world and new world Phasmatodea: Phylogenomics resolve the evolutionary history of stick and leaf insects. *Front. Ecol. Evol.* **7**, 1–14 (2019).
37. S. Bradler, J. A. Robertson, M. F. Whiting, A molecular phylogeny of Phasmatodea with emphasis on Necrosiinae, the most species-rich subfamily of stick insects. *Syst. Entomol.* **39**, 205–222 (2014).
38. J. A. Robertson, S. Bradler, M. F. Whiting, Evolution of oviposition techniques in stick and leaf insects (Phasmatodea). *Front. Ecol. Evol.* **6**, 1–15 (2018).
39. N. Cliquennois, Révision des Anisacanthidae, famille endémique de phasmes de Madagascar (Phasmatodea: Bacilloidea). *Ann. Soc. Entomol. Fr.* **44**, 59–85 (2008).
40. E. Tihelka, C. Cai, M. Giacomelli, D. Pisani, P. C. J. Donoghue, Integrated phylogenomic and fossil evidence of stick and leaf insects (Phasmatodea) reveal a Permian-Triassic co-origination with insectivores. *R. Soc. Open Sci.* **7**, 201689 (2020).
41. S. Bank, S. Bradler, A second view on the evolution of flight in stick and leaf insects (Phasmatodea). *BMC Ecol. Evol.* **22**, 1–17 (2022).
42. M. Chavent, V. Kuentz-Simonet, A. Labenne, J. Saracco, Multivariate analysis of mixed data: The R package PCAmixdata. arXiv [Preprint] (2017). <https://arxiv.org/abs/1411.4911> (Accessed 5 March 2024).
43. S. Bank *et al.*, A tree of leaves: Phylogeny and historical biogeography of the leaf insects (Phasmatodea: Phylliidae). *Commun. Biol.* **4**, 1–12 (2021).
44. M. Muschick, A. Indermaur, W. Salzburger, Convergent evolution within an adaptive radiation of cichlid fishes. *Curr. Biol.* **22**, 2362–2368 (2012).
45. S. Datta, S. Datta, Methods for evaluating clustering algorithms for gene expression data using a reference set of functional classes. *BMC Bioinf.* **7**, 1–9 (2006).
46. E. E. Williams, "The origin of faunas. Evolution of lizard congeners in a complex island fauna: A trial analysis" in *Evolutionary Biology*, T. Dobzhansky, M. K. Hecht, W. C. Steere, Eds. Springer, US, 1972), pp. 47–89.
47. A. Liaw, M. Wiener, Classification and regression by randomForest. *R News* **2**, 18–22 (2002).
48. J. P. Huelsenbeck, R. Nielsen, J. P. Bollback, Stochastic mapping of morphological characters. *Syst. Biol.* **52**, 131–158 (2003).
49. J. P. Bollback, SIMMAP: Stochastic character mapping of discrete traits on phylogenies. *BMC Bioinf.* **7**, 88 (2006).
50. L. J. Revell, phytools: An R package for phylogenetic comparative biology (and other things). *Methods Ecol. Evol.* **3**, 217–223 (2012).
51. R. R. Junker, J. Kuppler, A. C. Bathke, M. L. Schreyer, W. Trutschnig, Dynamic range boxes—A robust nonparametric approach to quantify size and overlap of n-dimensional hypervolumes. *Methods Ecol. Evol.* **7**, 1503–1513 (2016).
52. B. Blonder *et al.*, hypervolume: High dimensional geometry, set operations, projection, and inference using kernel density estimation, support vector machines, and convex hulls. R package version 3.1.1 (2023). <https://CRAN.R-project.org/package=hypervolume>. Accessed 10 June 2023.
53. J. Clavel, G. Escarguel, G. Merceron, mvmorph: An R package for fitting multivariate evolutionary models to morphometric data. *Methods Ecol. Evol.* **6**, 1311–1319 (2015).
54. K. Arbuckle, C. M. Bennett, M. P. Speed, A simple measure of the strength of convergent evolution. *Methods Ecol. Evol.* **5**, 685–693 (2014).
55. K. Arbuckle, A. Minter, Windex: Analyzing convergent evolution using the wheatsheaf index in R. *Evol. Bioinf.* **2015**, 11–14 (2015).
56. D. M. Grossnickle *et al.*, Challenges and advances in measuring phenotypic convergence. *Evolution* **78**, 1355–1371 (2024), 10.1093/evolut/qpae081.
57. D. C. Collar, J. S. Reece, M. E. Alfaro, P. C. Wainwright, R. S. Mehta, Imperfect morphological convergence: Variable changes in cranial structures underlie transitions to durophagy in moray eels. *Am. Nat.* **183**, E168–E184 (2014).
58. D. C. Adams, M. L. Collyer, A general framework for the analysis of phenotypic trajectories in evolutionary studies. *Evolution* **63**, 1143–1154 (2009).
59. D. I. Bolnick, R. D. H. Barrett, K. B. Oke, D. J. Rennison, Y. E. Stuart, (Non)Parallel evolution. *Annu. Rev. Ecol. Syst.* **49**, 303–330 (2018).
60. M. Lässig, V. Mustonen, A. M. Walczak, Predicting evolution. *Nat. Ecol. Evol.* **1**, 1–9 (2017).
61. M. T. Wortel *et al.*, Towards evolutionary predictions: Current promises and challenges. *Evol. Appl.* **16**, 3–21 (2023).
62. T. Leinonen, R. J. S. McCairns, G. Herczeg, J. Merilä, Multiple evolutionary pathways to decreased lateral plate coverage in freshwater threespine sticklebacks. *Evolution* **66**, 3866–3875 (2012).
63. E. B. Rosenblum, C. E. Parent, E. E. Brandt, The molecular basis of phenotypic convergence. *Annu. Rev. Ecol. Syst.* **45**, 203–229 (2014).
64. J. F. Storz, Causes of molecular convergence and parallelism in protein evolution. *Nat. Rev. Genet.* **17**, 239–250 (2016).
65. A. J. Verster, A. K. Ramani, S. J. McKay, A. G. Fraser, Comparative RNAi screens in *C. elegans* and *C. briggsae* reveal the impact of developmental system drift on gene function. *PLoS Genet.* **10**, e1004077 (2014).
66. S. Bank *et al.*, Reconstructing the nonadaptive radiation of an ancient lineage of ground-dwelling stick insects (Phasmatodea: Heteropterygidae). *Syst. Entomol.* **46**, 487–507 (2021).
67. Y. M. Pacheco, *Ecomorph Convergence in Stick Insects (Phasmatodea) with Emphasis on the Lonchodinae of Papua New Guinea* (Brigham Young University, 2018).
68. R. Bouckaert *et al.*, BEAST 2: A software platform for Bayesian evolutionary analysis. *PLoS Comput. Biol.* **10**, e1003537 (2014).
69. S. A. Price *et al.*, Building a body shape morphospace of teleostean fishes. *Integr. Comp. Biol.* **59**, 716–730 (2019).
70. L. J. Revell, Size-correction and principal components for interspecific comparative studies. *Evolution* **63**, 3258–3268 (2009).
71. G. Brock, V. Pihur, S. Datta, S. Datta, cValid: An R package for cluster validation. *J. Stat. Softw.* **25**, 1–22 (2008).
72. D. C. Adams, M. L. Collyer, Phylogenetic comparative methods and the evolution of multivariate phenotypes. *Annu. Rev. Ecol. Syst.* **50**, 405–425 (2019).
73. R. P. Boisseau, S. Bradler, D. J. Emlen, Data from "Divergence time and environmental similarity predict the strength of morphological convergence in stick and leaf insects" Zenodo. <https://doi.org/10.5281/zenodo.13774069>. Deposited 17 September 2024.